Benjamin N. Ediger,[1,2] Aiping Du,[1] Jingxuan Liu,[1] Chad S. Hunter,[3] Erik R. Walp,[1] Jonathan Schug,[4] Klaus H. Kaestner,[4] Roland Stein,[3] Doris A. Stoffers,[2] and Catherine L. May[1,5,6]

Islet-1 Is Essential for Pancreatic β-Cell Function

Diabetes 2014;63:4206–4217 | DOI: 10.2337/db14-0096

Islet-1 (Isl-1) is essential for the survival and ensuing differentiation of pancreatic endocrine progenitors. Isl-1 remains expressed in all adult pancreatic endocrine lineages; however, its specific function in the postnatal pancreas is unclear. Here we determine whether Isl-1 plays a distinct role in the postnatal β-cell by performing physiological and morphometric analyses of a tamoxifen-inducible, β-cell–specific *Isl-1* loss-of-function mouse: *Isl-1$^{L/L}$; Pdx1-CreER^{Tm}*. Ablating *Isl-1* in postnatal β-cells reduced glucose tolerance without significantly reducing β-cell mass or increasing β-cell apoptosis. Rather, islets from *Isl-1$^{L/L}$; Pdx1-CreER^{Tm}* mice showed impaired insulin secretion. To identify direct targets of Isl-1, we integrated high-throughput gene expression and Isl-1 chromatin occupancy using islets from *Isl-1$^{L/L}$; Pdx1-CreER^{Tm}* mice and βTC3 insulinoma cells, respectively. Ablating *Isl-1* significantly affected the β-cell transcriptome, including known targets *Insulin* and *MafA* as well as novel targets *Pdx1* and *Slc2a2*. Using chromatin immunoprecipitation sequencing and luciferase reporter assays, we found that Isl-1 directly occupies functional regulatory elements of *Pdx1* and *Slc2a2*. Thus Isl-1 is essential for postnatal β-cell function, directly regulates *Pdx1* and *Slc2a2*, and has a mature β-cell cistrome distinct from that of pancreatic endocrine progenitors.

Compromised pancreatic β-cell function is a critical factor underlying the onset of diabetes (1). β-Cell functional capacity is regulated by extrinsic signaling pathways and an intrinsic network of transcription factors (2,3). It is established that β-cell–specific transcription factors like MafA and Pdx1 are essential components of this intrinsic transcriptional network (4–7). It is less clear how pan-endocrine transcription factors like Islet-1 (Isl-1) affect postnatal β-cell function. These factors are expressed in all postnatal pancreatic endocrine cell types, suggesting roles in general endocrine function, cell type–specific physiology, or both. The majority of in vivo studies investigating pan-endocrine transcription factors have conditionally ablated their respective genes prior to maturation of the pancreatic endocrine compartment (8–11). As a result, it remains unclear whether these factors have unique functional roles in the endocrine cell types of the postnatal pancreas. To this point, a recent study demonstrated that the pan-endocrine factor NeuroD1 is necessary for maintaining functional maturity of mouse β-cells (12). Given these findings, Isl-1 and other pan-endocrine transcription factors may have functional roles in the postnatal β-cell distinct from their well-established developmental roles.

Isl-1 is a Lin11, Isl-1, and Mec-3 homeodomain (LIM-HD) factor that is essential for the genesis of the dorsal pancreatic bud at E9.5, the survival of Pax6^{+} endocrine progenitors at E13.5, and the ensuing maturation of α-, β-, δ-, and pancreatic polypeptide (PP) cells (11,13). Isl-1 was identified as an *Insulin* enhancer binding protein (14) and was subsequently shown to directly interact with NeuroD1 to promote *Insulin* expression (15). While Isl-1 expression is conserved in a variety of adult neuroendocrine cell types (16), many of the identified Isl-1 target genes are associated with pancreatic endocrine function, including *IAPP*,

[1]Department of Pathology and Laboratory Medicine, Children's Hospital of Philadelphia, Philadelphia, PA
[2]Department of Medicine and Institute for Diabetes, Obesity, and Metabolism, Perelman School of Medicine, University of Pennsylvania, Philadelphia, PA
[3]Department of Molecular Physiology and Biophysics, Vanderbilt University Medical Center, Nashville, TN
[4]Department of Genetics and Institute for Diabetes, Obesity, and Metabolism, Perelman School of Medicine, University of Pennsylvania, Philadelphia, PA
[5]Department of Pathology and Laboratory Medicine, Perelman School of Medicine, University of Pennsylvania, Philadelphia, PA
[6]Janssen Research & Development, Spring House, PA

Corresponding authors: Catherine L. May, catheril@mail.med.upenn.edu, and Doris A. Stoffers, stoffers@mail.med.upenn.edu.

Received 17 January 2014 and accepted 11 July 2014.

This article contains Supplementary Data online at http://diabetes.diabetesjournals.org/lookup/suppl/doi:10.2337/db14-0096/-/DC1.

D.A.S. and C.L.M. contributed equally to this study.

© 2014 by the American Diabetes Association. Readers may use this article as long as the work is properly cited, the use is educational and not for profit, and the work is not altered.

Sst, *Gcg*, and *Kcnj11/Kir6.2* (11,17–21). In adult mouse β-cells, Isl-1 was identified as a key downstream target of leptin-induced Janus kinase signal transducer and activator of transcription 3 signaling (22). Recently, a transgenic mouse with islet-specific overexpression of *Isl-1* displayed improved β-cell function (23). Interest in the mechanisms whereby Isl-1 regulates postnatal β-cell function is further raised by type 2 diabetes linkage and genome-wide association studies that identified genetic markers in the chromosomal region encompassing the *ISL-1* locus (24–27).

Despite genetic links to type 2 diabetes in humans and evidence that Isl-1 regulates key genes associated with pancreatic function, the in vivo requirement for Isl-1 in postnatal β-cell function has not been thoroughly investigated. Here we derived an inducible, β-cell–specific, *Isl-1* loss-of-function mouse. By combining microarray analysis of Isl-1–deficient islets with Isl-1 chromatin immunoprecipitation (ChIP) sequencing (ChIP-Seq) of βTC3 mouse insulinoma cells, we constructed the transcriptional network controlled by Isl-1 and identified novel gene targets directly regulated by Isl-1 in postnatal β-cells.

RESEARCH DESIGN AND METHODS

Animals

The *Isl-1*$^{L/L}$ and *Pdx1-CreER*^{Tm} mouse lines have been previously described (28,29). Mice were maintained on a mixed C57BL/6, CD1, and Sv129 background. The morning after birth was considered P0.5. Analysis was restricted to female mice. Tamoxifen (Tm; Sigma-Aldrich, T5648) at 50 μg/g mouse bodyweight was administered to 8-week-old mice via three intraperitoneal injections at 24-h intervals. Tm was dissolved in 90% sunflower seed oil (vehicle [Veh]; volume for volume), 10% ethanol (volume for volume). Unless otherwise stated, analysis of Tm-treated animals was performed 2 days after the third injection. The Children's Hospital of Philadelphia Institutional Use and Care Committees approved all animal studies.

Immunohistochemical and Immunofluorescence Analyses

Pancreata were dissected, fixed in 4% paraformaldehyde (pH 7.0) for 6 h at 25°C, and embedded in paraffin or optimal-cutting-temperature compound (Tissue-Tek, 4583). Sections were blocked using CAS-Block (Invitrogen, 008120), and primary antibodies were applied overnight at 4°C. Primary and secondary antisera information is provided in Supplementary Tables 1 and 2, respectively. For immunofluorescence, Vectashield mounting medium with DAPI (Vector, H-1200) was used to counterstain nuclei, and fluorescein isothiocyanate tyramide signal amplification (PerkinElmer, NEL741001KT) was used for Isl-1 detection. For immunohistochemistry, signal was detected using Vectastain Elite ABC Kit (standard; Vector, PK-6100) and DAB Peroxidase Substrate Kit (Vector, SK-4100). Staining was visualized using a Leica DM6000 B microscope, and images were captured using the Leica LAS AF software and Leica DFC300 FX digital camera.

To quantify staining, slides were digitally scanned using an Aperio ScanScope CS2 or MetaMorph microscopy automation software and analyzed using ImageScope software. Isl-1 ablation efficiency for a hormone$^+$ population was calculated as the percentage of Isl-1$^+$, hormone$^+$ cells per total hormone$^+$ cells using Indica Laboratories image analysis algorithms. β-Cell mass was calculated by averaging the percentage of insulin-stained tissue area over three sections that were taken at 100 μm levels. The fraction of positive area was then multiplied by the wet mass of the dissected pancreas measured at tissue harvest. Terminal deoxynucleotidyl TUNEL was performed as described (30) on three sections taken at 40 μm from pancreata that were harvested 14 days after the first Tm injection. These sections were then costained for insulin. TUNEL$^+$, insulin$^+$ cells were counted manually and normalized to the number of total β-cells. The number of total β-cells was determined by counting the Nkx6.1$^+$ nuclei on an adjacent section.

RNA Isolation, cDNA Synthesis, Quantitative PCR, and Microarray

Total RNA was extracted from pancreatic islets isolated by the standard collagenase P (Roche, 11 213 873 001) protocol (31) or whole pancreata. Total RNA preparation and cDNA synthesis were performed as described (23). Quantitative PCR (qPCR) reactions were performed using SYBR Green JumpStart Taq ReadyMix (Sigma-Aldrich, S4438) and a Stratagene Mx3005P qPCR system. Fold enrichment of mRNA message was calculated by normalizing to a reference gene (see Supplementary Table 3 for qPCR primers). Control and mutant-isolated islet total RNA extractions were matched for pancreatic endocrine purity as described (32). Microarray analysis was performed by the University of Pennsylvania's Diabetes Research Center Functional Genomics Core. RNA was labeled with the Agilent Low Input Kit and hybridized, using a dye-switch design, to the Agilent 4 × 44K Whole Mouse Genome Microarray. Arrays were hybridized overnight and scanned using the Agilent Microarray Scanner. Data were normalized using normalizeBetweenArrays from the Limma package followed by SAMR to identify differentially expressed genes.

Western Blot Analysis

Western blots were performed as described (33) using isolated islet whole-cell lysates. Pdx1 (Santa Cruz, Pdx1 sc-14664, 1:200) and α-tubulin (Sigma-Aldrich, T5168, 1:3000) antisera were used.

Glucose and Hormone Assays

Plasma glucose and insulin were measured as described (23). Random-fed plasma glucose was assessed between 10:00 and 11:00 A.M. Glucose tolerance and glucose-stimulated plasma insulin levels were assessed as described (11). Isolated islet glucose-stimulated insulin secretion (GSIS) was assessed via static incubations using 20–50 islets of similar size as described (23). Values for islet insulin content and secretion were normalized to the total number of islets per incubation. Values for relative islet insulin secretion reflect

islet insulin secretion normalized to islet insulin content. Mouse insulin concentration was determined by ELISA (Mercodia, 10–1247). Pancreatic insulin content was measured as described (11).

ChIP and ChIP-Seq

βTC3 insulinoma cells were grown in monolayer (~4×10^6 cells), or mouse islets were isolated from CD1 mice. ChIP assays were performed as described (33). Normal mouse IgG (Santa Cruz, SC2025) and anti–Isl-1 (Hybridoma Bank UI, 39.4D5-C) were used to immunoprecipitate sheared chromatin. Enrichment was determined using qPCR. Values are presented as fold enrichment over normal mouse IgG. To account for background, values were normalized to enrichment at the *Pepck* locus, which is not bound by Isl-1. For ChIP primers, see Supplementary Table 3. Whole-genome ChIP-Seq analysis using anti–Isl-1 (Hybridoma Bank UI, 39.4D5-C) to immunoprecipitate sheared βTC3 chromatin was performed as described in conjunction with University of Pennsylvania's Diabetes Research Center Functional Genomics Core (33).

Electrophoretic Mobility Shift Assays

Electrophoretic mobility shift assays (EMSAs) were performed as described using a *pCS2-Isl-1-Myc* plasmid (gift from Dr. Pfaff) as a template for in vitro translation (11). The radiolabeled probe was designed as *MafA*-Region 3 (11). Competition experiments were performed using 100-fold molar excess of unlabeled dsDNA oligonucleotides spanning the homeodomain binding elements (HBEs) in *Pdx1* enhancer areas I, II, and IV. For dsDNA oligonucleotide sequences see Supplementary Table 4. Supershift analysis was performed as described using a cocktail of Isl-1 antisera (Hybridoma Bank UI, 39.3F7, 39.4D5, 40.2D6, and 40.3A4) or anti-Myc (Santa Cruz, sc-40) (11).

Luciferase Vector Construction and Reporter Assays

Sequences of interest were cloned into the *pGL4.27* luciferase vector (Promega). To create HBE mutations, site-directed mutants were generated as described (33). Luciferase reporter assays were performed in βTC3 or HeLa as described (33). Exogenous Isl-1 protein was overexpressed using the *pCS2-Isl-1-Myc* vector. Transient transfection of all vectors was accomplished using Lipofectamine 2000 (Invitrogen). All *pCR4-TOPO* and *pGL4.27* vectors containing wild-type or HBE-mutated *Pdx1* area I, II, and IV and *Slc2a2* Re1 and Re2 are available upon request.

RESULTS

Isl-1$^{L/L}$; Pdx1-CreER^{Tm} Mice Exhibit a Baseline Level of Postnatal *Isl-1* Ablation Prior to Administering Tm

To determine the functional requirement for Isl-1 in the postnatal β-cell, we derived an inducible, β-cell–specific, *Isl-1* loss-of-function mouse model (*Isl-1$^{L/L}$; Pdx1-CreER^{Tm}*). Because of a recent report demonstrating minimal Tm-independent recombination of the *Rosa26* locus in *Pdx1-CreER^{Tm}* transgenic mice (34), we assessed baseline Isl-1 protein and transcript levels before administering Tm to 8-week-old female *Isl-1$^{L/L}$; Pdx1-CreER^{Tm}* mice, hereon notated as *Isl-1$^{L/L}$; Pdx1-CreER^{Tm}$_{(No\ Tm)}$*. Isl-1 immunohistochemistry in 8-week-old *Isl-1$^{L/L}$; Pdx1-CreER^{Tm}$_{(No\ Tm)}$* animals revealed pancreatic islets with multiple Isl-1$^-$ nuclei (Fig. 1*A* and *B*). When quantified, *Isl-1$^{L/L}$; Pdx1-CreER^{Tm}$_{(No\ Tm)}$* mice had a 20% decrease in Isl-1$^+$ nuclei compared with controls (Fig. 1*C*). Using qPCR, we determined that the relative *Isl-1* mRNA transcript was reduced by ~38% in islets isolated from *Isl-1$^{L/L}$; Pdx1-CreER^{Tm}$_{(No\ Tm)}$* animals; however, this difference was not statistically significant (Fig. 1*D*).

Despite a reduction in Isl-1$^+$ β-cells, gross pancreatic morphology, islet distribution, and insulin staining were indistinguishable between 8-week-old *Isl-1$^{L/L}$; Pdx1-CreER^{Tm}$_{(No\ Tm)}$* animals and controls (Fig. 1*E* and *F* and data not shown). Importantly, β-cell mass in 8-week-old *Isl-1$^{L/L}$; Pdx1-CreER^{Tm}$_{(No\ Tm)}$* pancreata, as reflected by insulin$^+$ staining, was equivalent to that of age-matched controls (Fig. 1*G*). Despite maintaining normal β-cell mass, 8-week-old *Isl-1$^{L/L}$; Pdx1-CreER^{Tm}$_{(No\ Tm)}$* animals displayed reduced first-phase insulin secretion in response to acute glucose challenge (Fig. 1*H*). In 4-week-old *Isl-1$^{L/L}$; Pdx1-CreER^{Tm}$_{(No\ Tm)}$* animals, we also observed a moderate impairment of in vivo GSIS that was associated with mild glucose intolerance (Supplementary Fig. 1*A* and *B*). Intriguingly, 8-week-old Tm-treated *Isl-1$^{L/+}$; Pdx1-CreER^{Tm}* mice did not display glucose tolerance defects (Supplementary Fig. 1*C*), suggesting that Isl-1 is haplosufficient in the β-cell, and any pathophysiological defects reflect complete *Isl-1* ablation in the β-cell. Together, these control experiments demonstrate that the *Pdx1-CreER^{Tm}* strain directs limited, Tm-independent recombination of *Isl-1* as early as 4 weeks of age.

Isl-1 is required for the differentiation and maturation of pancreatic endocrine precursors (11). Conditionally ablating Isl-1 in the pancreatic epithelium at E13.5 results in mice that are born without a mature endocrine compartment, are hyperglycemic by P7, and die between 3 and 8 weeks of age (11). Significant Tm-independent recombination of the *Isl-1* locus during embryogenesis could confound analysis of postnatal animals. However, insulin$^+$, Isl-1$^-$ cells were rarely detected by coimmunofluorescence at P0.5 in pancreata from *Isl-1$^{L/L}$$_{(No\ Tm)}$* or *Isl-1$^{L/L}$; Pdx1-CreER^{Tm}$_{(No\ Tm)}$* animals (Supplementary Fig. 2*A* and *B*). We also determined that the level of pancreatic *Isl-1* transcript at P0.5 was indistinguishable between *Isl-1$^{L/L}$$_{(No\ Tm)}$* and *Isl-1$^{L/L}$; Pdx1-CreER^{Tm}$_{(No\ Tm)}$* animals (Supplementary Fig. 2*C*). At P5, *Isl-1$^{L/L}$; Pdx1-CreER^{Tm}$_{(No\ Tm)}$* mice displayed normal random-fed plasma glucose, their endocrine compartment was present, and gross pancreatic morphology and intraislet hormone distribution appeared normal (Supplementary Fig. 2*D–F*). Furthermore, *Isl-1$^{L/L}$; Pdx1-CreER^{Tm}$_{(No\ Tm)}$* animals showed no signs of morbidity (data not shown). These observations contrast with previously characterized mouse models that ablate *Isl-1* in the developing pancreas (11,13). Altogether, *Isl-1$^{L/L}$; Pdx1-CreER^{Tm}$_{(No\ Tm)}$* animals have no evidence

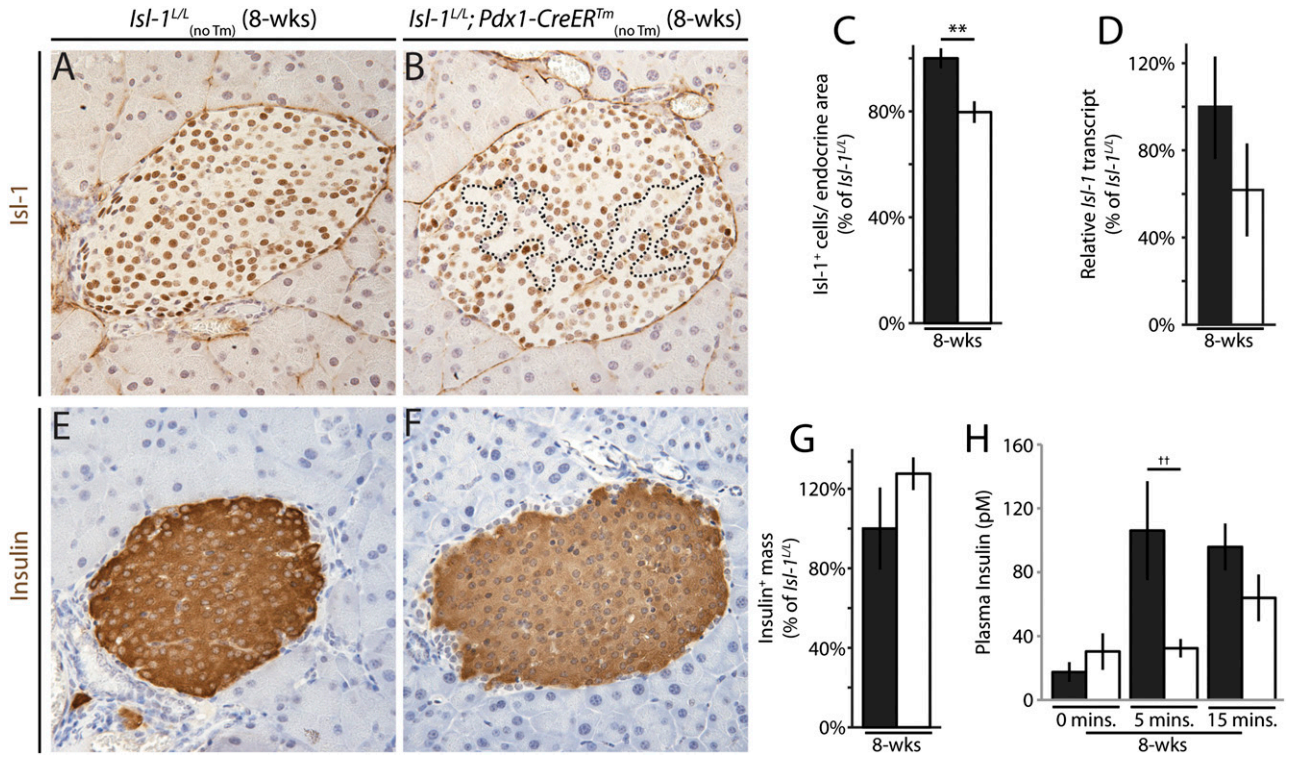

Figure 1—Partial ablation of *Isl-1* in *Isl-1$^{L/L}$; Pdx1-CreER^{Tm}$_{(No\ Tm)}$* animals prior to Tm administration impairs response to acute glucose challenge. *A* and *B*: Isl-1 immunohistochemistry of 8-week-old female islets (20×). In *B*, the dotted lines highlight major, contiguous areas of Isl-1 paucity. *C*: Quantification of Isl-1$^+$ nuclei per pancreatic endocrine area in 8-week-old females ± SEM (n = 5 per genotype; P = 0.00627). *D*: *Isl-1* mRNA levels relative to *Actin* transcript using total RNA extracts from 8-week-old female isolated islets ± SEM (n = 5 per genotype). *E* and *F*: Insulin immunohistochemistry of 8-week-old female islets (20×). *G*: Insulin$^+$ mass of 8-week-old females ± SEM (n = 5 per genotype). *H*: Plasma insulin levels of 8-week-old females after intraperitoneal glucose bolus following a 16-h fast ± SEM (*Isl-1$^{L/L}$$_{(No\ Tm)}$*, n = 4; *Isl-1$^{L/L}$; Pdx1-CreER^{Tm}$_{(No\ Tm)}$*, n = 6). In *C*, *D*, *G*, and *H*, black bars represent *Isl-1$^{L/L}$$_{(No\ Tm)}$* animals and white bars represent *Isl-1$^{L/L}$; Pdx1-CreER^{Tm}$_{(No\ Tm)}$* animals. Values for *C*, *D*, and *G* are presented as percentage of the *Isl-1$^{L/L}$$_{(No\ Tm)}$* animals. Analysis with two-way Student t test, $^{**}P < 0.01$. Analysis with repeated measures, two-way ANOVA with Bonferroni posttest, $\dagger\dagger P < 0.01$.

of significant Tm-independent recombination during pancreas development.

Ablating *Isl-1* in β-Cells Impairs Glucose Tolerance and Insulin Secretion Without Impacting β-Cell Mass

To maximally ablate *Isl-1* in adult β-cells, we administered Tm to 8-week-old *Isl-1$^{L/L}$; Pdx1-CreER^{Tm}* and control *Isl-1$^{L/L}$* animals, respectively notated *Isl-1$^{L/L}$; Pdx1-CreER^{Tm}$_{IP(Tm)}$* and *Isl-1$^{L/L}$$_{IP(Tm)}$* (Fig. 2*A*). The 5-day pulse-chase recombined most remaining β-cell *Isl-1* alleles. *Isl-1* mRNA expression in islets isolated from *Isl-1$^{L/L}$; Pdx1-CreER^{Tm}$_{IP(Tm)}$* animals was consistently reduced to ∼24% of *Isl-1$^{L/L}$$_{IP(Tm)}$* levels (Fig. 2*B*). A similar result was observed with Isl-1 immunostaining; almost all insulin$^+$ cells lacked Isl-1 expression (Fig. 2*C*–*E*). The majority of the remaining Isl-1$^+$ nuclei were located at the periphery of the islet where non–β-cell endocrine cell types (i.e., α-, δ-, ε-, and PP cells) are typically located in mouse islets (Fig. 2*C*–*D*). Accordingly, Isl-1 was not ablated in α-cells; however, Isl-1 was ablated in a significant percentage of δ-cells (Fig. 2*C*–*E* and Supplementary Fig. 2*G* and *H*), paralleling Pdx1 expression in adult δ-cells (35).

When compared with *Isl-1$^{L/L}$$_{IP(Tm)}$* animals, *Isl-1$^{L/L}$; Pdx1-CreER^{Tm}$_{IP(Tm)}$* mice had increased random-fed plasma glucose levels but maintained equivalent random-fed insulin levels (Fig. 2*F* and *G*). Following fasting, *Isl-1$^{L/L}$; Pdx1-CreER^{Tm}$_{IP(Tm)}$* mice displayed a robust glucose intolerance phenotype and impaired GSIS response (Fig. 2*H* and *I*). In agreement with our findings in the postnatal *Isl-1$^{L/L}$; Pdx1-CreER^{Tm}$_{(No\ Tm)}$* animals (Fig. 1 and Supplementary Fig. 1), the Veh-treated *Isl-1$^{L/L}$; Pdx1-CreER^{Tm}$_{IP(Veh)}$* animals also displayed a moderate but significant glucose tolerance phenotype (Fig. 2*H*). Within only 5 days, maximally ablating *Isl-1* noticeably exacerbated the *Isl-1$^{L/L}$; Pdx1-CreER^{Tm}$_{IP(Veh)}$* glucose intolerance and GSIS phenotypes. Unlike 8-week-old *Isl-1$^{L/L}$; Pdx1-CreER^{Tm}$_{(No\ Tm)}$* animals (Fig. 1*H*), both the first and the second phase of the GSIS response were significantly reduced in *Isl-1$^{L/L}$; Pdx1-CreER^{Tm}$_{IP(Tm)}$* mice (Fig. 2*I*).

Isl-1 has been implicated as a survival factor in developing cell populations, including pancreatic endocrine progenitors (11,36,37). A substantial and rapid reduction in β-cell mass could account for the physiological defects observed in the *Isl-1$^{L/L}$; Pdx1-CreER^{Tm}$_{IP(Tm)}$* animals;

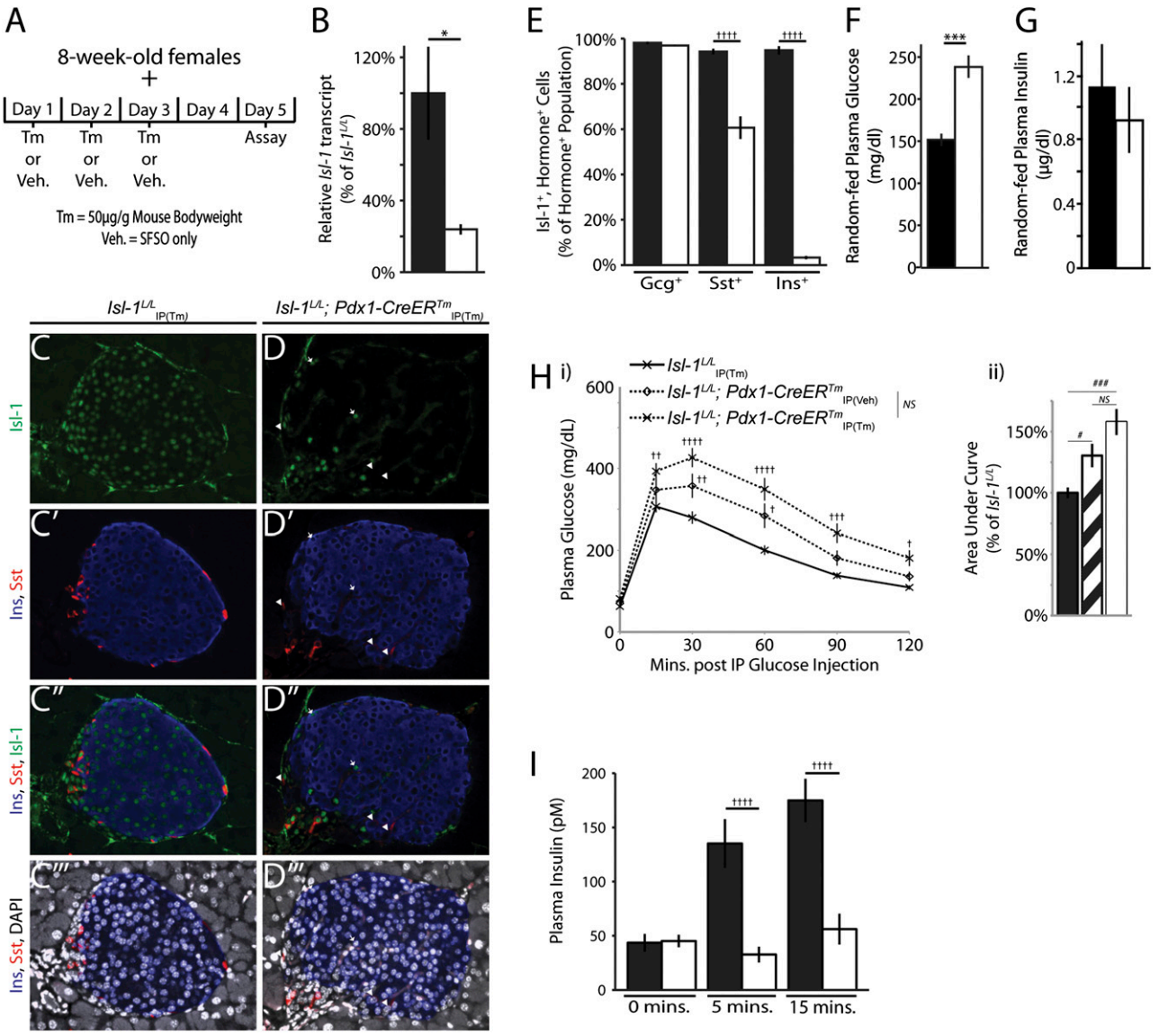

Figure 2—Maximal ablation of Isl-1 in the adult animal impairs insulin secretion. *A*: The Tm-administration schedule for 8-week-old female animals. Three sequential intraperitoneal injections of Tm (50 μg/g of mouse bodyweight) or Veh (sunflower seed oil) were administered at 24-h intervals followed by a 2-day chase. *B*: *Isl-1* mRNA expression relative to *Actin* using total RNA extracts from isolated islets as percentage of *Isl-1*$^{L/L}$$_{IP(Tm)}$ animals ± SEM (*Isl-1*$^{L/L}$$_{IP(Tm)}$, $n = 4$; *Isl-1*$^{L/L}$; *Pdx1-CreER*^{Tm}$_{IP(Tm)}$, $n = 4$; $P = 0.027$). *C* and *D*: Coimmunofluorescence for insulin, somatostatin, Isl-1, and DAPI (20×). *D*: White arrowheads indicate Isl-1^{-}, somatostatin^{+} cells, and white arrows indicate residual Isl-1^{+}, insulin^{+} cells. *E*: Isl-1 ablation efficiency in glucagon^{+}, somatostatin^{+}, and insulin^{+} cell populations ± SEM ($n = 4$ per genotype). *F*: Random-fed plasma glucose ± SEM (*Isl-1*$^{L/L}$$_{IP(Tm)}$, $n = 5$; *Isl-1*$^{L/L}$; *Pdx1-CreER*^{Tm}$_{IP(Tm)}$, $n = 8$; $P = 0.0006$). *G*: Random-fed plasma insulin ± SEM ($n = 8$ per genotype). *H*: *i*) Intraperitoneal glucose tolerance test performed after 16-h fast. The solid line with crosshairs represents *Isl-1*$^{L/L}$$_{IP(Tm)}$, the dashed line with crosshairs represents *Isl-1*$^{L/L}$; *Pdx1-CreER*^{Tm}$_{IP(Tm)}$, and the dashed line with open diamonds represents *Isl-1*$^{L/L}$; *Pdx1-CreER*^{Tm}$_{IP(Veh)}$. Values are presented as ± SEM (*Isl-1*$^{L/L}$$_{IP(Tm)}$, $n = 12$; *Isl-1*$^{L/L}$; *Pdx1-CreER*^{Tm}$_{IP(Tm)}$, $n = 10$; *Isl-1*$^{L/L}$; *Pdx1-CreER*^{Tm}$_{IP(Veh)}$, $n = 7$). *H*: *ii*) Integrated area under intraperitoneal glucose tolerance test curves as percentage of *Isl-1*$^{L/L}$$_{IP(Tm)}$ ± SEM. *I*: Plasma insulin levels in response to acute intraperitoneal glucose bolus after 16-h fast ± SEM (*Isl-1*$^{L/L}$$_{IP(Tm)}$, $n = 10$; *Isl-1*$^{L/L}$; *Pdx1-CreER*^{Tm}$_{IP(Tm)}$, $n = 8$). In *B* and *E–I*, black bars represent *Isl-1*$^{L/L}$$_{IP(Tm)}$, black and white striped bars represent *Isl-1*$^{L/L}$; *Pdx1-CreER*^{Tm}$_{IP(Veh)}$, and white bars represent *Isl-1*$^{L/L}$; *Pdx1-CreER*^{Tm}$_{IP(Tm)}$. Analysis with two-way Student *t* test, *$P < 0.05$; ***$P < 0.001$. Analysis with one-way ANOVA and Tukey posttest, #$P < 0.05$; ###$P < 0.001$. Analysis with repeated measures, two-way ANOVA, and Bonferroni posttest, †$P < 0.05$; ††$P < 0.01$; †††$P < 0.001$; ††††$P < 0.0001$. Gcg^{+}, glucagon^{+}; Ins^{+}, insulin^{+}; Ins, insulin; IP, intraperitoneal; NS, no significance; SFSO, sunflower seed oil; Sst, somatostatin; Sst^{+}, somatostatin^{+}.

however, there was no difference in the number of insulin^{+}, TUNEL^{+} cells between *Isl-1*$^{L/L}$; *Pdx1-CreER*^{Tm}$_{IP(Tm)}$ and *Isl-1*$^{L/L}$$_{IP(Tm)}$ animals (Fig. 3*A–C*), and β-cell mass was not significantly reduced (Fig. 3*D*). Taken together, these analyses demonstrate that the glucose homeostasis defects in *Isl-1*$^{L/L}$; *Pdx1-CreER*^{Tm}$_{IP(Tm)}$ mice are not due to a significant increase in β-cell apoptosis or a substantial reduction in β-cell mass.

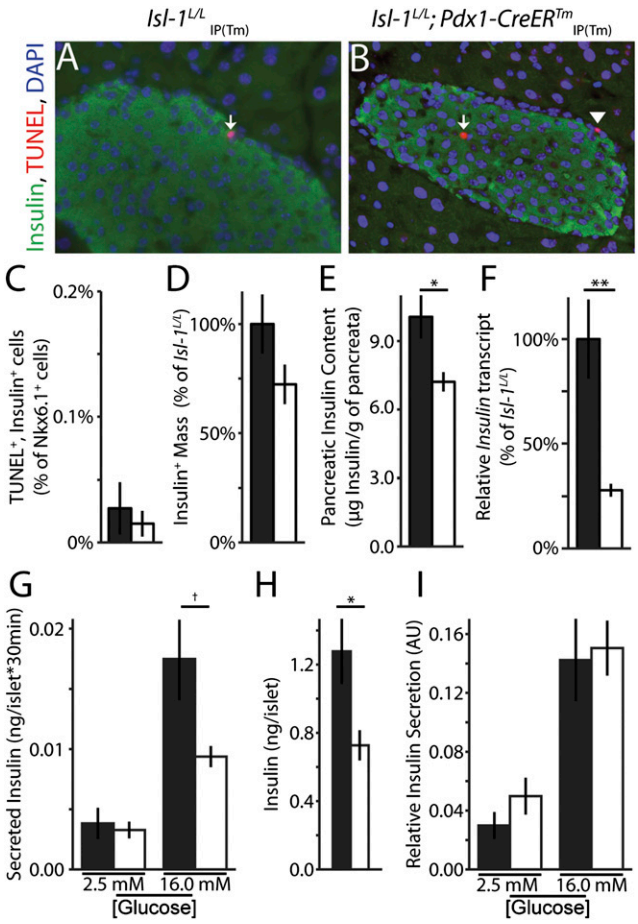

Figure 3—Ablation of Isl-1 reduces pancreatic insulin content but does not increase β-cell apoptosis. *A* and *B*: TUNEL, insulin, and DAPI shown by coimmunofluorescence (40×). TUNEL assays were performed on pancreatic sections from animals 14 days after first Tm injection. White arrows point to TUNEL$^+$, insulin$^+$ cells, and the white arrowhead points to a TUNEL$^+$, insulin$^-$ cell. *C*: Insulin$^+$, TUNEL$^+$ cells as a percentage of total Nkx6.1$^+$ β-cells ± SEM (n = 4 per genotype). *D*: Quantification of insulin$^+$ mass ± SEM (*Isl-1*$^{L/L}$$_{IP(Tm)}$, n = 6; *Isl-1*$^{L/L}$; *Pdx1-CreER*^{Tm}$_{IP(Tm)}$, n = 8). *E*: Quantification of pancreatic insulin content ± SEM (*Isl-1*$^{L/L}$$_{IP(Tm)}$, n = 6; *Isl-1*$^{L/L}$; *Pdx1-CreER*^{Tm}$_{IP(Tm)}$, n = 8; P = 0.0482). *F*: Quantification of *Insulin* mRNA expression relative to *Hprt* using total RNA extracts from isolated islets ± SEM (*Isl-1*$^{L/L}$$_{IP(Tm)}$, n = 6; *Isl-1*$^{L/L}$; *Pdx1-CreER*^{Tm}$_{IP(Tm)}$, n = 8; $P = 5.57 \times 10^{-3}$). *G*: Static incubation of isolated islets in glucose at 2.5 and 16.0 mmol/L ± SEM (*Isl-1*$^{L/L}$$_{IP(Tm)}$, n = 6; *Isl-1*$^{L/L}$; *Pdx1-CreER*^{Tm}$_{IP(Tm)}$, n = 8). Insulin secretion was normalized to islet number. *H*: Insulin content of islets used in static incubations ± SEM (*Isl-1*$^{L/L}$$_{IP(Tm)}$, n = 6; *Isl-1*$^{L/L}$; *Pdx1-CreER*^{Tm}$_{IP(Tm)}$, n = 8; P = 0.014). *I*: Relative islet insulin secretion where islet insulin secretion was normalized to islet insulin content ± SEM. Values for *D* and *F* are presented as percentage of *Isl-1*$^{L/L}$$_{IP(Tm)}$ animals. In *C–I*, black bars represent *Isl-1*$^{L/L}$$_{IP(Tm)}$ and white bars represent *Isl-1*$^{L/L}$; *Pdx1-CreER*^{Tm}$_{IP(Tm)}$. Analysis with two-way Student t test, *$P < 0.05$; **$P < 0.01$. Analysis with two-way ANOVA and Bonferroni posttest, †$P < 0.05$.

We observed a 25% reduction in total pancreatic insulin content in *Isl-1*$^{L/L}$*; Pdx1-CreER*^{Tm}$_{IP(Tm)}$ mice (Fig. 3*E*). Since Isl-1 has been demonstrated to regulate *Insulin* transcription (14,15), we quantified the level of total *Insulin* mRNA in isolated islets and observed a 75% reduction in *Isl-1*$^{L/L}$*; Pdx1-CreER*^{Tm}$_{IP(Tm)}$ animals (Fig. 3*F*). Reduced pancreatic insulin content and islet *Insulin* transcripts without increased apoptosis prompted us to investigate the functional capacity of islets. To directly evaluate islet function, we isolated islets from *Isl-1*$^{L/L}$*; Pdx1-CreER*^{Tm}$_{IP(Tm)}$ and *Isl-1*$^{L/L}$$_{IP(Tm)}$ animals and performed static incubation assays with basal and stimulatory glucose concentrations (2.5 and 16.0 mmol/L). In response to 16.0 mmol/L glucose, islets from *Isl-1*$^{L/L}$*; Pdx1-CreER*^{Tm}$_{IP(Tm)}$ animals secreted less insulin than islets isolated from *Isl-1*$^{L/L}$$_{IP(Tm)}$ animals (Fig. 3*G*). However, the insulin content per islet was also significantly depleted in *Isl-1*$^{L/L}$*; Pdx1-CreER*^{Tm}$_{IP(Tm)}$ animals (Fig. 3*H*). When we normalized islet secretion to islet content, the relative insulin secretion rate of *Isl-1*$^{L/L}$$_{IP(Tm)}$ and *Isl-1*$^{L/L}$*; Pdx1-CreER*^{Tm}$_{IP(Tm)}$ islets was similar at both 2.5 and 16.0 mmol/L glucose (Fig. 3*I*). Overall, our data demonstrate that ablating Isl-1 in the adult β-cell impairs glucose homeostasis and compromises β-cell insulin secretion primarily as a result of reduced insulin synthesis.

The Isl-1 Cistrome of the Mature β-Cell Is Distinct From That of the Developing Pancreatic Epithelium

To assess the gene expression changes occurring in Isl-1–deficient β-cells, a microarray was performed using RNA isolated from *Isl-1*$^{L/L}$*; Pdx1-CreER*^{Tm}$_{IP(Tm)}$ and *Isl-1*$^{L/L}$$_{IP(Tm)}$ islets. This analysis yielded 714 genes whose expression was significantly altered (Fig. 4*A*, Supplementary Fig. 3*A*, and Supplementary Table 5). We used Ingenuity Systems software to perform gene ontology (GO) analysis of this data set. Not surprisingly, genes involved in "glucose tolerance" and "quantity of insulin in the blood" were significantly enriched among affected genes (Fig. 4*B*). Interestingly, GO categories associated with aspects of neuroendocrine function were also distinguished through this analysis, including genes regulating hormone concentration, intracellular molecular transport, and secretion of molecules (Fig. 4*B*). To determine if any of these differentially expressed genes were direct targets of Isl-1 in the mature β-cell, we performed Isl-1 ChIP-Seq using chromatin extracted from mouse βTC3 insulinoma cells (βTC3 cells) (Supplementary Table 6). Meta-analysis was performed using the microarray and ChIP-Seq data sets to determine putative targets of Isl-1 transcriptional regulation (Fig. 4*A* and Supplementary Fig. 3*A*). From this analysis, we identified *MafA*, a known regulatory target of Isl-1 (11), as well as *Slc2a2*, the gene encoding the Glut2 glucose transporter essential for rodent β-cell GSIS. We confirmed downregulation of MafA and Slc2a2 at both the transcript and the protein level in islets isolated from *Isl-1*$^{L/L}$*; Pdx1-CreER*^{Tm}$_{IP(Tm)}$ animals (Fig. 4*C–G*).

Gene network analysis of our microarray data set utilizing Ingenuity Systems software yielded a de novo network containing factors essential for β-cell function (Fig. 4*H*). This gene network included both *MafA* and *Slc2a2*. *Pdx1* appeared in this network and was also identified in the ChIP-Seq. Intriguingly, *Pdx1* was not

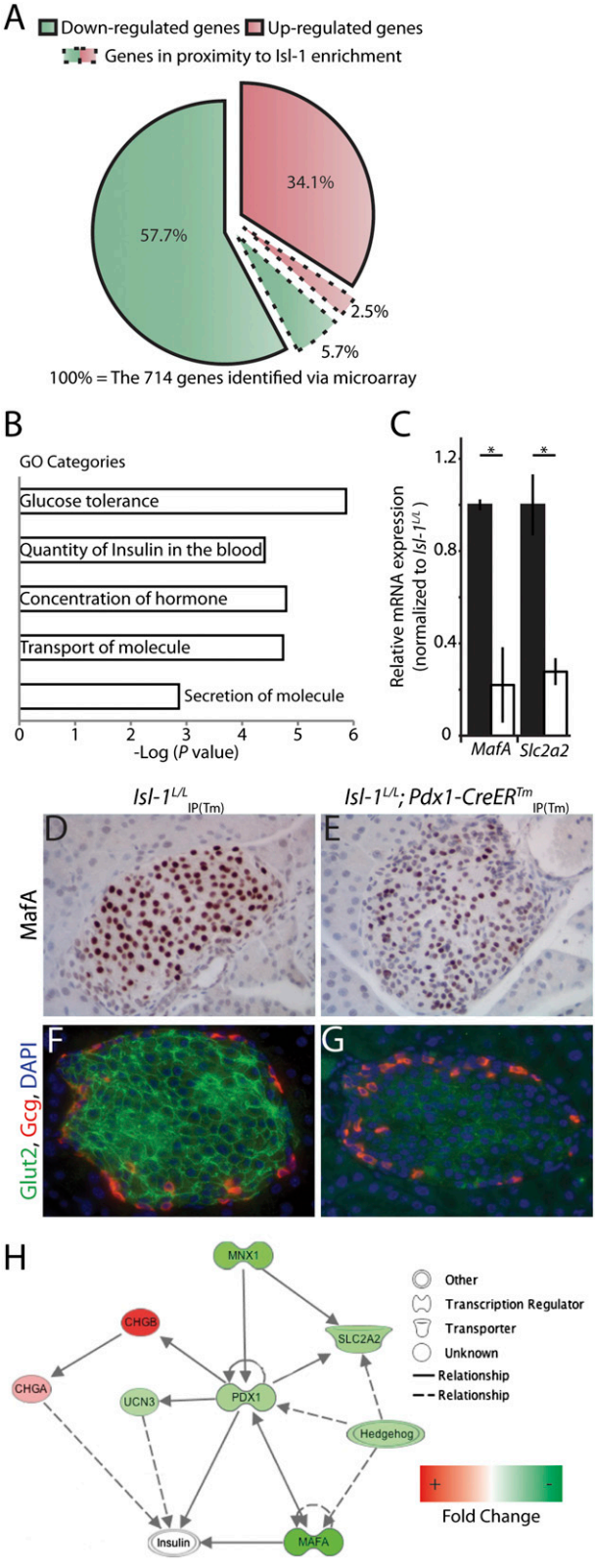

Figure 4—Ablating Isl-1 significantly alters the pancreatic islet transcriptome. *A*: Exploded pie chart representing genes identified by microarray with significant expression differences in *Isl-1*$^{L/L}$; *Pdx1-CreER*$^{Tm}_{IP(Tm)}$ animals. The red and green partitions represent genes that were, respectively, up- and downregulated. Partitions outlined with the dashed lines represent genes in 100 kb proximity to areas of Isl-1 enrichment identified by the Isl-1 βTC3 insulinoma ChIP-Seq. Values are presented as a percentage of all 714 significantly misregulated genes identified in the microarray. *B*: Selected biological processes that were enriched in gene ontology analysis of the microarray data set. Values are presented as $-\log_{10}$ (*P* value). *C*: *MafA* and *Slc2a2* mRNA expression relative to *Hprt* ± SEM (*Isl-1*$^{L/L}_{IP(Tm)}$, $n = 6$; *Isl-1*$^{L/L}$; *Pdx1-CreER*$^{Tm}_{IP(Tm)}$, $n = 8$). Values are normalized by gene to the relative expression in *Isl-1*$^{L/L}_{IP(Tm)}$ animals. Black bars represent *Isl-1*$^{L/L}_{IP(Tm)}$, and white bars = *Isl-1*$^{L/L}$; *Pdx1-CreER*$^{Tm}_{IP(Tm)}$. Analysis with two-way Student *t* test, $^*P < 0.05$. *D* and *E*: Visualization of MafA using immunohistochemistry (20×). *F* and *G*: Visualization of Glut2 and glucagon using coimmunofluorescence (20×). *H*: De novo network generated from gene network analysis of *Isl-1*$^{L/L}$; *Pdx1-CreER*^{Tm} microarray data set. Red and green highlights indicate statistically significant up- and downregulation, respectively; intensity of highlight corresponds to fold change. White highlight indicates factors that were not identified by the microarray. Solid arrows and dashed arrows represent confirmed and suspected regulatory relationships, respectively. Gcg, glucagon; GO, gene ontology.

differentially regulated when *Isl-1* was conditionally ablated from the mouse pancreatic epithelium at E13.5 (11). In *Isl-1*$^{L/L}$; *Pdx1-CreER*$^{Tm}_{IP(Tm)}$ animals, however, Pdx1 was by this time significantly downregulated at both the transcript and protein levels (Fig. 5*A* and *B*) to a degree commensurate with the pathophysiological reductions in Pdx1 protein previously described in heterozygous *Pdx1* loss-of-function mutants (38). The *cis*-regulatory regions (areas I, II, III, and IV) for *Pdx1* have been well characterized (Fig. 5*C*) (39,40). Statistical analysis of the Isl-1 βTC3 ChIP-Seq identified three peaks that corresponded to *Pdx1* areas I, II, and IV (Fig. 5*C*). To confirm the peak-calling analysis, we performed Isl-1 ChIP followed by qPCR using chromatin extracted from βTC3 cells (Fig. 5*D*) and from CD1 mouse islets (Fig. 5*E*).

To determine if Isl-1 binds to putative HBEs (i.e., TAAT/ATTA-containing regions) within *Pdx1* areas I, II, and IV, we performed EMSAs using Myc-tagged Isl-1 incubated with a ^{32}P-radiolabeled *MafA*-Region-3 (Reg3) probe (Fig. 5*F*). Competition assays were performed using unlabeled oligonucleotide probes representing the putative Isl-1 sites within *Pdx1* areas I, II, and IV. At least one competitor from each tested *Pdx1* enhancer successfully reduced Isl-1 binding to *MafA*-Reg3. To determine if the HBEs within the bound competitors were required for *Pdx1* expression, we performed luciferase reporter assays in βTC3 cells. Vectors containing the wild-type sequences of *Pdx1* areas I, II, or IV elicited significant signal above the empty vector (Fig. 5*G*). From the oligonucleotides that successfully competed with the *MafA*-Reg3 probe, we selected one oligomer from each *Pdx1* enhancer element: area I-4, area II-3, and area IV-4. While we saw no change in signal when mutating HBE area I-4, we did see a significant decrease in signal when either HBE area II-3 or area IV-4 was mutated (Fig. 5*G*). Lastly, we performed a luciferase reporter assay using the Pdx1-area II vector in HeLa cells. Exogenously overexpressed Isl-1 amplified wild-type Pdx1-area II vector reporter activity (Fig. 5*H*).

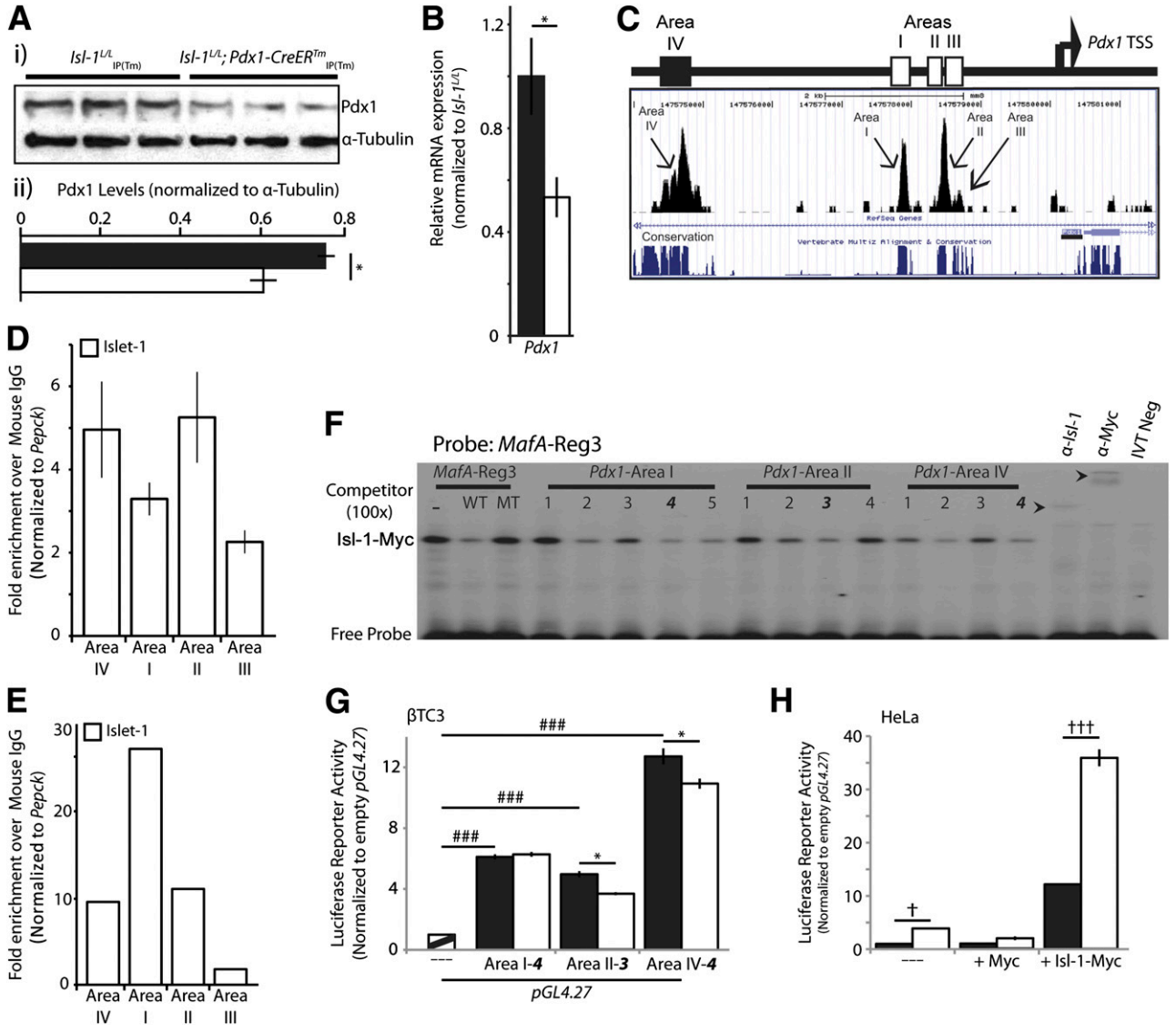

Figure 5— Isl-1 directly regulates Pdx1. *A*: *i*) Western blot for Pdx1 and α-tubulin using protein lysates of isolated islets. *A*: *ii*) Quantification of Pdx1 normalized to α-tubulin ± SEM ($n = 3$ per genotype; $P = 0.01222$). *B*: Relative mRNA expression of *Pdx1* to *Hprt* ± SEM (*Isl-1*$^{L/L}$ $_{IP(Tm)}$, $n = 6$; *Isl-1*$^{L/L}$; *Pdx1-CreER*^{Tm} $_{IP(Tm)}$, $n = 8$). Values are normalized to relative expression in *Isl-1*$^{L/L}$ $_{IP(Tm)}$ animals. In *A ii*) and *B*, black bars represent *Isl-1*$^{L/L}$ $_{IP(Tm)}$ and white bars represent *Isl-1*$^{L/L}$; *Pdx1-CreER*^{Tm} $_{IP(Tm)}$. *C*: A scaled schematic of the *Pdx1* genomic locus. The known *Pdx1* regulatory domains areas I, II, and III are represented by white boxes and area IV by a black box. The *Pdx1* transcription start site is indicated by the arrow. UCSC mouse genome browser of the *Pdx1* genomic locus annotated with βTC3 chromatin Isl-1 ChIP-Seq and vertebrate Multiz alignment in black; the *Pdx1* transcription start site is underlined. Arrows highlight Isl-1 enrichment at the four described *Pdx1* regulatory elements. *D*: Isl-1 ChIP using chromatin extracted from βTC3 cells ± SEM ($n = 3$). *E*: Isl-1 ChIP using chromatin extracted from isolated islets ($n = 1$). Values in both *D* and *E* are presented as fold enrichment over normal mouse IgG after first normalizing to the inactive *Pepck* locus. *F*: EMSA using recombinant Myc-tagged Isl-1 protein. The Isl-1 binding site at *MafA*-Reg3 was used as the radiolabeled probe. Control competition assays were performed with wild-type and mutated *MafA*-Reg3 oligo probes. Competition assays were also performed using oligonucleotides representing putative HBEs in *Pdx1*-areas I, II, and IV. Competitors were added at 100× free probe concentration. Supershifts using both antibodies against Isl-1 and Myc were observed. A protein:DNA complex was not observed in the absence of recombinant Isl-1-Myc protein. Bold, italicized enumeration corresponds to selected HBEs for mutational analysis. *G*: Luciferase assay for putative Isl-1 HBEs in *Pdx1* enhancers using βTC3 cells. Values are normalized to empty *pGL4.27* vector ± SEM ($n = 3$). The black and white striped bar represents empty vector. Vector inserts correspond to the selected HBEs in *F*. The black bars represent wild-type sequences. The white bars represent mutational ablation of the putative HBE. *H*: Luciferase assay for *Pdx1* area II in HeLa cells. Values are normalized to empty *pGL4.27* vector ± SEM ($n = 3$). White and black bars represent cells transfected using *pGL4.27* with and without the *Pdx1* area II insert, respectively. Analysis with two-way Student *t* test, $^*P < 0.05$. Analysis with one-way ANOVA and Tukey posttest, $^{###}P < 0.001$. Analysis with two-way ANOVA and Bonferroni posttest, $^{\dagger}P < 0.05$, $^{\dagger\dagger\dagger}P < 0.001$. IVT Neg, in vitro translation negative; TSS, transcription start site.

Taken together, these experiments suggest that Isl-1 directly regulates the adult β-cell expression of *Pdx1* through at least areas II and IV.

Isl-1 Directly Regulates *Slc2a2A* Through the Downstream Re2 Enhancer Element

Although previous work using βTC3 cells demonstrated that Isl-1 was enriched at two putative *Slc2a2 cis*-regulatory elements (Re1 and Re2) (Fig. 6*A*), *Slc2a2* expression was unaltered in *Isl-1*$^{L/L}$*; Pdx1-Cre* mice, a model that ablated *Isl-1* in the pancreatic epithelium at E13.5 (11,21). Thus *Slc2a2* represents another key β-cell gene that is putatively regulated by Isl-1 only in the mature β-cell. To further determine whether Re1 and Re2 are involved in mediating *Slc2a2* expression, we used a luciferase reporter in βTC3 cells. Luciferase activity in βTC3 cells was only observed using the reporter plasmid containing Re2. Furthermore, Isl-1 overexpression was sufficient to increase the Re2-containing vector reporter activity (Fig. 6*B*). The *Slc2a2*-Re2 sequence is highly conserved when compared with rat and human genomes (Fig. 6*C*). Within Re2, five putative HBEs were identified (Fig. 6*C*), and mutational analysis of *Slc2a2*-Re2 sites 1, 2, and 5 reduced the reporter activity, whereas similar treatment to site 4 enhanced activity (Fig. 6*D*). Overall, this analysis strongly supports the notion that Isl-1 directly regulates *Slc2a2* through *cis*-regulatory elements in *Slc2a2*-Re2.

DISCUSSION

To determine the requirement for Isl-1 in the postnatal β-cell, we used a Tm-inducible, β-cell-specific, loss-of-function mouse model. Ablating *Isl-1* in the postnatal β-cell impaired glucose tolerance and GSIS without affecting β-cell survival. Moreover, loss of Isl-1 compromised β-cell insulin secretion and altered the islet transcriptome. By combining microarray and ChIP-Seq analysis, we constructed a β-cell transcriptional network for Isl-1. Meta-analysis of this network identified new direct transcriptional targets of Isl-1, including *Slc2a2*, the glucose transporter that mediates a critical upstream step in mouse β-cell GSIS, and *Pdx1*, an essential transcriptional regulator of postnatal β-cell function. Remarkably, both *Slc2a2* and *Pdx1* are regulated by Isl-1 in the postnatal β-cell but not in pancreatic endocrine progenitors.

This study also exposed a limitation of the *Pdx1-CreER*^{Tm} line. When crossed to *Rosa-lacZ* mice, the *Pdx1-CreER*^{Tm} line displayed negligible Tm-independent recombination (34). In our *Isl-1*$^{L/L}$*; Pdx1-CreER*^{Tm} mice, however, we encountered a significantly greater degree of Tm-independent *Isl-1* recombination. We demonstrated that this occurred postnatally and that our analysis was not confounded by developmental deletion of *Isl-1*. Notably, 8-week-old *Isl-1*$^{L/+}$*; Pdx1-CreER*$^{Tm}{}_{\mathrm{IP(Tm)}}$ animals displayed no phenotype. Therefore, the phenotype in the *Isl-1*$^{L/L}$*; Pdx1-CreER*$^{Tm}{}_{\mathrm{(No\ Tm)}}$ mice reflected the accumulation of β-cells with two recombined *Isl-1* alleles. Overall, increased surveillance for postnatal Tm-independent recombination with appropriate controls is warranted when using the *Pdx1-CreER*^{Tm} line.

Previous in vitro studies have identified that *Isl-1* regulates genes associated with pancreatic endocrine function but have not provided definitive insights into the requirement for Isl-1 in the adult endocrine pancreas (17–20). Following postnatal deletion of Isl-1, we observed decreased β-cell function without increased apoptosis. In line with these observations, transgenic mice overexpressing *Isl-1* in the endocrine pancreas increased β-cell function without enhanced β-cell proliferation (23). Considering the established relationship between Isl-1 and *Insulin* transcription (14,15,22), these in vivo findings further demonstrate that Isl-1 is essential for β-cell functional capacity. Nonetheless, our findings are at odds with the observation that overexpression and knockdown of *Isl-1* in ex vivo rat islets enhanced β-cell proliferation and apoptosis, respectively (41). We speculate that the apoptosis/proliferation phenotypes observed in rat islets are secondary to Isl-1–regulating β-cell function or that the insults of islet isolation and culture may have unveiled a prosurvival function of Isl-1 in β-cells.

It is becoming increasingly evident that specified β-cells undergo a final period of maturation before attaining complete physiological capacity (42). Our findings suggest that the requirement for Isl-1 in postnatal versus developing β-cells is distinct. While ablating *Isl-1* in endocrine progenitors had no effect on fetal levels of *Slc2a2* and *Pdx1* (11,21), we demonstrate here that ablating *Isl-1* in postnatal β-cells reduces expression of both genes. Distinct roles for a transcription factor in developing versus postnatal β-cells have been observed for MafA and NeuroD1 (5,43). Similarly, Arx is necessary for the establishment of α-cell fate during pancreas development but is dispensable for maintaining α-cell fate even though its expression is maintained (44). Determining what regulates these shifts in transcriptional influence will be essential in defining immature versus mature pancreatic endocrine cells.

Observing that Isl-1 directly regulates *MafA* and *Pdx1* in postnatal β-cells is also noteworthy when considering the plasticity of the adult pancreatic endocrine compartment (42). Multiple studies have demonstrated that misexpression of *MafA* and *Pdx1* is sufficient to drive expression of β-cell–specific genes in non–β-cells (6,45,46). Isl-1 also directly regulates *Arx*, a transcription factor necessary for directing α-cell fate (33,44). Since α-, β-, δ-, and PP cells appear to arise from a common progenitor pool (42), ubiquitous expression of Isl-1 in the adult endocrine pancreas suggests that regulatory mechanisms exist to restrict Isl-1 transcriptional targets among the pancreatic endocrine lineages. It is well established that LIM-HD transcription factors drive cell-fate decisions in progenitor populations by activating distinct expression profiles (47). This is accomplished by LIM domain binding (Ldb) adaptor proteins nucleating combinatoric, multimeric LIM-HD complexes (48,49). The

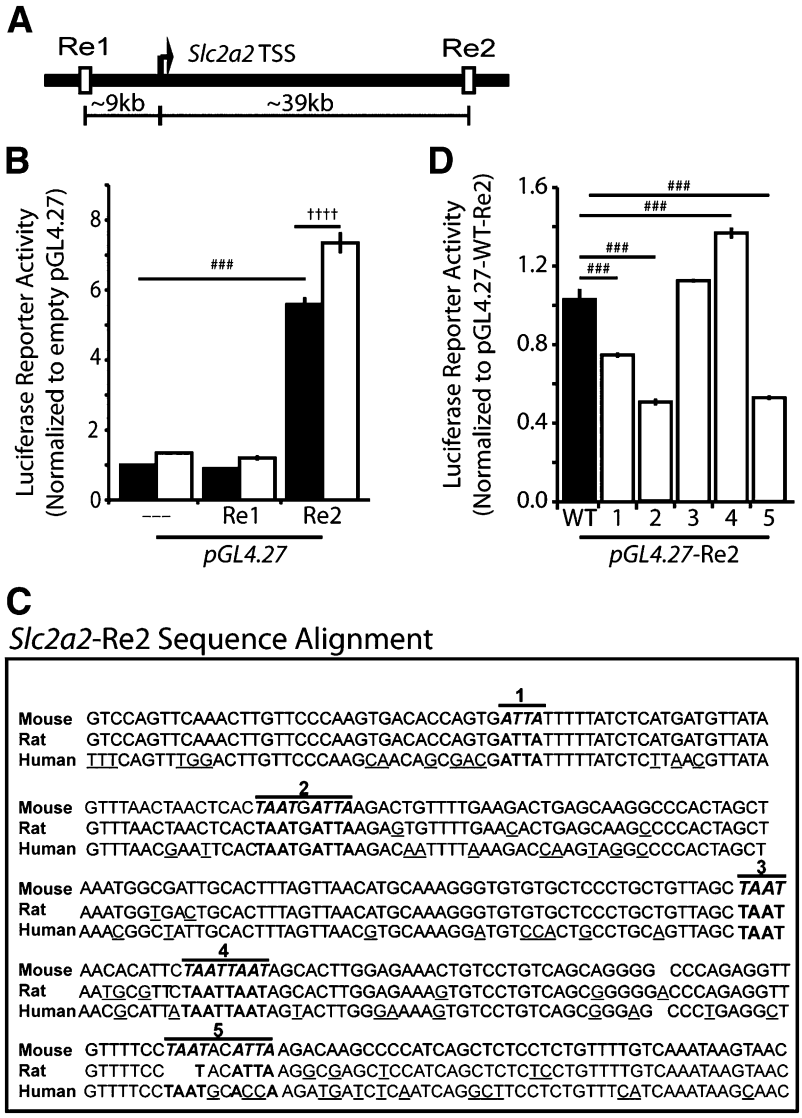

Figure 6—Isl-1 directly regulates Slc2a2. *A*: A schematic of the genomic *Slc2a2* locus. White boxes represent putative enhancer elements, Re1 and Re2. Re1 and Re2 are ~9 kb upstream and 39 kb downstream of the *Slc2a2* transcription start site, respectively. *B*: Luciferase assay for putative *Slc2a2* enhancer elements using βTC3 cells. Values are normalized to empty *pGL4.27* vector ± SEM (n = 3). Black and white bars represent βTC3 cells with and without overexpression of Isl-1-Myc, respectively. *C*: *Slc2a2*-Re2 sequence alignment for mouse, rat, and human. Base pairs that differ from the mouse sequence are underlined. Putative HBEs are bold and italic in the mouse sequence and bold in both rat and human sequences. The five putative HBEs are enumerated 1–5. *D*: Luciferase assay for putative Isl-1 binding sites in *Slc2a2*-Re2 using βTC3 cells. Values are normalized to *pGL4.27* vector containing wild-type *Slc2a2*-Re2 ± SEM (n = 3). The black bar represents wild-type *Slc2a2*-Re2. The white bars represent vectors containing *Slc2a2*-Re2 with mutational ablation of the respective putative HBE. Analysis with one-way ANOVA and Tukey posttest, ###$P < 0.001$. Analysis with two-way ANOVA and Bonferroni posttest, ††††$P < 0.0001$. TSS, transcription start site; WT, wild type.

building blocks for this mechanism are still expressed in the adult endocrine pancreas. Ldb1, like Isl-1, is ubiquitously expressed in the adult endocrine pancreas, and other members of the LIM-HD family of transcription factors in addition to Isl-1 are enriched in islets as well, including Lhx1 and Mnx1/Hb9 (21,50). The epigenetic landscapes of the pancreatic endocrine cell types may also play role in restricting Isl-1 regulatory targets. For instance, Dnmt1-mediated DNA methylation is required to maintain β-cell identity, in part, by repressing *Arx* transcription (51). Similarly, mapping histone epigenetic modifications has identified variable enrichment of activating and repressive marks at cell type–specific genes between human α- and β-cells (52). Moving forward, it will be of great interest to determine which of these mechanisms contribute to directing the Isl-1 cistrome in the distinct endocrine lineages that populate the adult pancreas.

Acknowledgments. The authors thank the members of the Molecular Pathology & Imaging Core (MPIC) in the Penn Center for Molecular Studies in

Digestive and Liver Diseases (P30-DK050306), the Pathology Core Laboratory at the Children's Hospital of Philadelphia Research Institute, and the Radioimmunoassay/Biomarkers Core of the Penn Diabetes Research Center (P30-DK19525) for sample processing. The authors also thank the members of the Functional Genomics Core of the Penn Diabetes Research Center (P30-DK-19525) for performing sequencing and data analysis. The authors are also grateful for the *Pdx1-CreER^{Tm}* and *Isl-1$^{L/L}$* mice provided by Drs. Douglas Melton (Harvard University) and Sylvia Evans (University of California, San Diego), respectively.

Funding. This work was supported by DK078606, DK019525, and JDRF 2-2007-730 to C.L.M.; R01 DK068157 to D.A.S.; and DK078606 to R.S. B.N.E. was supported by T32-GM07229 and T32-HD007516-15, and C.S.H. was supported by DK007061 and DK083160.

Duality of Interest. No potential conflicts of interest relevant to this article were reported.

Author Contributions. B.N.E. researched the data and wrote the manuscript. A.D., J.L., and E.R.W. researched the data. C.S.H. researched the data and reviewed and edited the manuscript. J.S. and K.H.K. aided in generation and meta-analysis of high-throughput data and reviewed the manuscript. R.S., D.A.S., and C.L.M. supervised the research and wrote the manuscript. C.L.M. and D.A.S. are the guarantors of this work and, as such, had full access to all the data in the study and take responsibility for the integrity of the data and the accuracy of the data analysis.

Prior Presentation. Parts of this study were presented at the European Molecular Biology Organization/European Molecular Biology Laboratory Symposium 2014, Translating Diabetes, Heidelberg, Germany, 30 April–3 May 2014; at Imaging the Pancreatic Beta Cell: 5th NIDDK Workshop, Bethesda, MD, 15–16 April 2013; and at Keystone Symposium: Advances in Islet Biology, Monterey, CA, 25–30 March 2012.

References

1. Weir GC, Bonner-Weir S. Five stages of evolving beta-cell dysfunction during progression to diabetes. Diabetes 2004;53(Suppl. 3):S16–S21
2. Prentki M, Nolan CJ. Islet beta cell failure in type 2 diabetes. J Clin Invest 2006;116:1802–1812
3. Melloul D, Marshak S, Cerasi E. Regulation of insulin gene transcription. Diabetologia 2002;45:309–326
4. Ahlgren U, Jonsson J, Jonsson L, Simu K, Edlund H. beta-cell-specific inactivation of the mouse Ipf1/Pdx1 gene results in loss of the beta-cell phenotype and maturity onset diabetes. Genes Dev 1998;12:1763–1768
5. Artner I, Hang Y, Mazur M, et al. MafA and MafB regulate genes critical to beta-cells in a unique temporal manner. Diabetes 2010;59:2530–2539
6. Hang Y, Stein R. MafA and MafB activity in pancreatic β cells. Trends Endocrinol Metab 2011;22:364–373
7. Babu DA, Deering TG, Mirmira RG. A feat of metabolic proportions: Pdx1 orchestrates islet development and function in the maintenance of glucose homeostasis. Mol Genet Metab 2007;92:43–55
8. Smith SB, Qu HQ, Taleb N, et al. Rfx6 directs islet formation and insulin production in mice and humans. Nature 2010;463:775–780
9. Gierl MS, Karoulias N, Wende H, Strehle M, Birchmeier C. The zinc-finger factor Insm1 (IA-1) is essential for the development of pancreatic beta cells and intestinal endocrine cells. Genes Dev 2006;20:2465–2478
10. Ashery-Padan R, Zhou X, Marquardt T, et al. Conditional inactivation of Pax6 in the pancreas causes early onset of diabetes. Dev Biol 2004;269:479–488
11. Du A, Hunter CS, Murray J, et al. Islet-1 is required for the maturation, proliferation, and survival of the endocrine pancreas. Diabetes 2009;58:2059–2069
12. Gu C, Stein GH, Pan N, et al. Pancreatic beta cells require NeuroD to achieve and maintain functional maturity. Cell Metab 2010;11:298–310
13. Ahlgren U, Pfaff SL, Jessell TM, Edlund T, Edlund H. Independent requirement for ISL1 in formation of pancreatic mesenchyme and islet cells. Nature 1997;385:257–260
14. Karlsson O, Thor S, Norberg T, Ohlsson H, Edlund T. Insulin gene enhancer binding protein Isl-1 is a member of a novel class of proteins containing both a homeo- and a Cys-His domain. Nature 1990;344:879–882
15. Zhang H, Wang WP, Guo T, et al. The LIM-homeodomain protein ISL1 activates insulin gene promoter directly through synergy with BETA2. J Mol Biol 2009;392:566–577
16. Thor S, Ericson J, Brännström T, Edlund T. The homeodomain LIM protein Isl-1 is expressed in subsets of neurons and endocrine cells in the adult rat. Neuron 1991;7:881–889
17. Wang M, Drucker DJ. Activation of amylin gene transcription by LIM domain homeobox gene isl-1. Mol Endocrinol 1996;10:243–251
18. Leonard J, Serup P, Gonzalez G, Edlund T, Montminy M. The LIM family transcription factor Isl-1 requires cAMP response element binding protein to promote somatostatin expression in pancreatic islet cells. Proc Natl Acad Sci U S A 1992;89:6247–6251
19. Wang M, Drucker DJ. The LIM domain homeobox gene isl-1 is a positive regulator of islet cell-specific proglucagon gene transcription. J Biol Chem 1995;270:12646–12652
20. Hashimoto T, Nakamura T, Maegawa H, Nishio Y, Egawa K, Kashiwagi A. Regulation of ATP-sensitive potassium channel subunit Kir6.2 expression in rat intestinal insulin-producing progenitor cells. J Biol Chem 2005;280:1893–1900
21. Hunter CS, Dixit S, Cohen T, et al. Islet α-, β-, and δ-cell development is controlled by the Ldb1 coregulator, acting primarily with the islet-1 transcription factor. Diabetes 2013;62:875–886
22. Chen J, Fu R, Cui Y, et al. LIM-homeodomain transcription factor Isl-1 mediates the effect of leptin on insulin secretion in mice. J Biol Chem 2013;288:12395–12405
23. Liu J, Walp ER, May CL. Elevation of transcription factor Islet-1 levels in vivo increases β-cell function but not β-cell mass. Islets 2012;4:199–206
24. Ehm MG, Karnoub MC, Sakul H, et al.; American Diabetes Association GENNID Study Group. Genetics of NIDDM. Genomewide search for type 2 diabetes susceptibility genes in four American populations. Am J Hum Genet 2000;66:1871–1881
25. Shimomura H, Sanke T, Hanabusa T, Tsunoda K, Furuta H, Nanjo K. Nonsense mutation of islet-1 gene (Q310X) found in a type 2 diabetic patient with a strong family history. Diabetes 2000;49:1597–1600
26. Wiltshire S, Hattersley AT, Hitman GA, et al. A genomewide scan for loci predisposing to type 2 diabetes in a U.K. population (the Diabetes UK Warren 2 Repository): analysis of 573 pedigrees provides independent replication of a susceptibility locus on chromosome 1q. Am J Hum Genet 2001;69:553–569
27. Yokoi N, Kanamori M, Horikawa Y, et al. Association studies of variants in the genes involved in pancreatic beta-cell function in type 2 diabetes in Japanese subjects. Diabetes 2006;55:2379–2386
28. Sun Y, Dykes IM, Liang X, Eng SR, Evans SM, Turner EE. A central role for Islet1 in sensory neuron development linking sensory and spinal gene regulatory programs. Nat Neurosci 2008;11:1283–1293
29. Gu G, Dubauskaite J, Melton DA. Direct evidence for the pancreatic lineage: NGN3+ cells are islet progenitors and are distinct from duct progenitors. Development 2002;129:2447–2457
30. Soleimanpour SA, Crutchlow MF, Ferrari AM, et al. Calcineurin signaling regulates human islet beta-cell survival. J Biol Chem 2010;285:40050–40059
31. Gupta RK, Vatamaniuk MZ, Lee CS, et al. The MODY1 gene HNF-4alpha regulates selected genes involved in insulin secretion. J Clin Invest 2005;115:1006–1015
32. Lantz KA, Vatamaniuk MZ, Brestelli JE, Friedman JR, Matschinsky FM, Kaestner KH. Foxa2 regulates multiple pathways of insulin secretion. J Clin Invest 2004;114:512–520
33. Liu J, Hunter CS, Du A, et al. Islet-1 regulates Arx transcription during pancreatic islet alpha-cell development. J Biol Chem 2011;286:15352–15360
34. Liu Y, Suckale J, Masjkur J, et al. Tamoxifen-independent recombination in the RIP-CreER mouse. PLoS ONE 2010;5:e13533

35. Guz Y, Montminy MR, Stein R, et al. Expression of murine STF-1, a putative insulin gene transcription factor, in beta cells of pancreas, duodenal epithelium and pancreatic exocrine and endocrine progenitors during ontogeny. Development 1995;121:11–18
36. Pfaff SL, Mendelsohn M, Stewart CL, Edlund T, Jessell TM. Requirement for LIM homeobox gene Isl1 in motor neuron generation reveals a motor neuron-dependent step in interneuron differentiation. Cell 1996;84:309–320
37. Shi Y, Zhao S, Li J, Mao B. Islet-1 is required for ventral neuron survival in Xenopus. Biochem Biophys Res Commun 2009;388:506–510
38. Sachdeva MM, Claiborn KC, Khoo C, et al. Pdx1 (MODY4) regulates pancreatic beta cell susceptibility to ER stress. Proc Natl Acad Sci U S A 2009;106:19090–19095
39. Gerrish K, Gannon M, Shih D, et al. Pancreatic beta cell-specific transcription of the pdx-1 gene. The role of conserved upstream control regions and their hepatic nuclear factor 3beta sites. J Biol Chem 2000;275:3485–3492
40. Gerrish K, Van Velkinburgh JC, Stein R. Conserved transcriptional regulatory domains of the pdx-1 gene. Mol Endocrinol 2004;18:533–548
41. Guo T, Wang W, Zhang H, et al. ISL1 promotes pancreatic islet cell proliferation. PLoS ONE 2011;6:e22387
42. Pan FC, Wright C. Pancreas organogenesis: from bud to plexus to gland. Dev Dyn 2011;240:530–565
43. Zhang C, Moriguchi T, Kajihara M, et al. MafA is a key regulator of glucose-stimulated insulin secretion. Mol Cell Biol 2005;25:4969–4976
44. Wilcox CL, Terry NA, Walp ER, Lee RA, May CL. Pancreatic α-cell specific deletion of mouse Arx leads to α-cell identity loss. PLoS ONE 2013;8:e66214
45. Zhou Q, Brown J, Kanarek A, Rajagopal J, Melton DA. In vivo reprogramming of adult pancreatic exocrine cells to beta-cells. Nature 2008;455:627–632
46. Nomura S, Nakamura T, Hashimoto T, et al. MafA differentiates rat intestinal cells into insulin-producing cells. Biochem Biophys Res Commun 2006;349:136–143
47. Song MR, Sun Y, Bryson A, Gill GN, Evans SM, Pfaff SL. Islet-to-LMO stoichiometries control the function of transcription complexes that specify motor neuron and V2a interneuron identity. Development 2009;136:2923–2932
48. Matthews JM, Visvader JE. LIM-domain-binding protein 1: a multifunctional cofactor that interacts with diverse proteins. EMBO Rep 2003;4:1132–1137
49. Bhati M, Lee C, Nancarrow AL, et al. Implementing the LIM code: the structural basis for cell type-specific assembly of LIM-homeodomain complexes. EMBO J 2008;27:2018–2029
50. Harrison KA, Thaler J, Pfaff SL, Gu H, Kehrl JH. Pancreas dorsal lobe agenesis and abnormal islets of Langerhans in Hlxb9-deficient mice. Nat Genet 1999;23:71–75
51. Dhawan S, Georgia S, Tschen SI, Fan G, Bhushan A. Pancreatic β cell identity is maintained by DNA methylation-mediated repression of Arx. Dev Cell 2011;20:419–429
52. Bramswig NC, Everett LJ, Schug J, et al. Epigenomic plasticity enables human pancreatic α to β cell reprogramming. J Clin Invest 2013;123:1275–1284